Neural networks to estimate bubble diameter and bubble size distribution of flotation froth surfaces

by R.H. Estrada-Ruiz* and R. Pérez-Garibay*

Synopsis

This work analyses a new approach to estimates bubble size distribution of froth surfaces using artificial neural networks (ANN). Also, the robustness of ANN to interpret images with illumination perturbations, produced by light problems or dirt attached to the window of the video camera is evaluated. The experimental work was carried out in a laboratory flotation column, instrumented with an image acquisition system. The images were processed making use of a perceptron model with a hidden layer, sigmoidal transfer function and unitary bias, and the ANN trained with a back propagation algorithm. The results of validation show that ANN are reliable for learning and producing generalized predictions of the froth mean bubble diameter and bubble size distribution, when the model is trained using a database that contains information on the illumination intensity.

Keywords: image analysis, neural networks, bubble diameter, bubble size distribution.

Introduction

In the last decades the interest in characterizing the froth surfaces in mineral flotation has been growing because this information allows one to monitor online the performance of the process. One of most important characteristics of the froth surface is the bubble size distribution.

The measurement of the bubble diameter or bubble diameter distribution of flotation froth surfaces is not a trivial problem and only a few algorithms designed to accomplish the task have been developed for this application. Evidently, bubble diameter distribution is more important than mean diameter, because with bubble diameter distribution it is possible to estimate the carrying capacity with a better approximation.

The measurement of the mean bubble diameter making use of conventional mathematics is a ordinary task, but to perform the job with a neural network model is less studied. For example, it is interesting to know what happens when the lens gets dirty and the light intensity of the image decreases. These issues are treated in this paper.

The aim of this paper is to study the use of ANN to estimate the mean bubble diameter and the bubble size distribution of mineralized froth surfaces, as well as to evaluate the robustness of these models under conditions of variable lighting intensity.

Background

Process optimization is the interest of several researchers devoted to studying image analysis techniques and vision sensors. Symonds and De Jager[1] and Woodburn *et al.*[2] reported the first work on vision sensors applied to flotation control. The aim of these studies was to identify the characteristics such as texture, morphology and colour, of flotation froths systematically. Unfortunately, their systems were not used online due to computing limitations.

Subsequently, Moolman *et al.*[3] studied the froth surface structure, and concluded that bubble size is one of most important characteristics of froth surfaces. Hargrave and Hall[4] concluded that froths with a small bubble size and a narrowed size distribution showed a higher grade and mass flow rate compared to froths with large bubbles and a wide size distribution. Holtham and Nguyen[5] presented a statistical approach using the texture spectrum method to measure both the bubble size and froth structure. They stated that froth structures can be related to variations in the performance of the flotation process. As a result of the studies conducted by the authors, texture spectrum also provided a simple means of estimating the average bubble size in a froth image.

A review of the literature related to neural network applications in artificial visual systems indicates that the utility of these

* *Cinvestav-IPN (Unidad Saltillo), Ramos Arizpe, Coahuila, México.*

 SA ISSN 0038–223X/3.00 + 0.00. Paper received Oct. 2008; revised paper received May 2009.

models relies on their ability for pattern recognition, since they simplify the computational complexity of image analysis, as the image preprocessing generates a process computationally intensive. In other applications, artificial neural networks have been used to complete complex tasks such as mineral identification (Thomson *et al.*[6]), and particle size estimation (Gupta *et al.*[7]). Shumsher and Daharam[8] demonstrated the potential of hybrid neural networks for online interpretation of froth images and flotation process control.

In comparison with the available methods for images analysis, ANN is a fast and efficient technique to compute digitalized images, offering best performance for continuous and generalized predictions; one inconvenience is the requirement for an extensive database for the training. A database is composed by a numerical matrix where each row (set of inputs) corresponds to one line of pixels of the image, and for each input knowledge of the respective output is needed (reference diameter).

Contrary to ANN advantages, some commercial software used for bubble size estimation (i.e. Image Pro Plus®, Vision library of MatLab®, Eclipse®), based on sequential analysis of pixels, suffer from a slow and heavy numerical computation process. There are several and well validated techniques, used by the above mentioned software, to measure bubbles diameter in bubbling reactors (Grau and Heiskanen[9]; Hernández-Aguilar *et al.*[10]). These techniques work adequately, for conditions where bubbles are close-to spheres and surrounded by continuous phase (i.e. bubbling zone of flotation cells).

Apparatus and experimental methodology

The experimental programme was carried out in a 4-inch diameter laboratory flotation column. Figure 1(a) shows the instrumentation of the column. For froth surface image acquisition, a video camera connected to a PC was installed at a column height of 120 cm. In addition, an adequate chamber was used for external light isolation. A 90-watt halogen lamp was placed overhead at 80 cm from the overflow, making an angle of 80° with respect to the surface of the froth. A photocell was installed inside the chamber to register any change in the lighting intensity. Figure 1(b) shows three images of the surface of mineralized froths, showing different bubble sizes.

Sphalerite was used as floating mineral, and the pulp was conditioned using methyl isobutyl carbinol as frother and sodium isopropyl xanthate as collector. Sodium hydroxide was used to regulate the pH of the flotation pulp. The frother was added to a volume of 40 ℓ of water, and the temperature was set at 30°C. Next, 10.44 kg of sphalerite was added to the solution, and the pH of the pulp was regulated to pH = 10. Subsequently, cupric sulphate was added to activate the sphalerite and the flotation pulp was conditioned for 15 minutes.

The test was initiated and all the flow rates were set to the desired values. To make sure that the process had reached steady state operation (i.e., closed circuit, that is, recycling both concentrate and tails to conditioning tank), the column was operated for a further 15 minutes before sampling of the feed, concentrate and tailings. To avoid any process disturbance, the feed rate was sampled at the end of the test. This is because the feed pump was tied to the automatic control loop of the froth level. A series of photographs was taken during each set of experiments to record the froth surface image. This procedure was repeated for the different froth depths tested.

The bubble diameter was indirectly varied by controlling bubble coalescence. This objective was attained by changing the hydrophobicity of the particles using different collector concentrations and by varying froth depth.

Image data acquisition and ANN learning

Froth images were taken with an acquisition frequency of 0.145 s, using a Matlab® library. Images were subsequently converted from colour (RGB) to gray scale images (BW). The Image Pro® software was used to obtain manual bubble diameter measurements, since the software is not capable of performing the task automatically, when bubbles are not isolated. This is the main reason for using ANN in the characterization of froth surfaces. Note that manual bubble diameter measurement becomes the reference mean diameter, which will be subsequently used as the pattern diameter during the ANN training. The first stage to obtain the reference diameter ($d_{b\ \text{average of image}}$) was to define the border of each bubble using a manual procedure, as shown in Figure 2(a). Once the bubble edge has been delineated (raised hand), the software computes the arithmetic mean diameter (see Figure 2(b)). This procedure was repeated for all the bubbles of the image to obtain the reference or

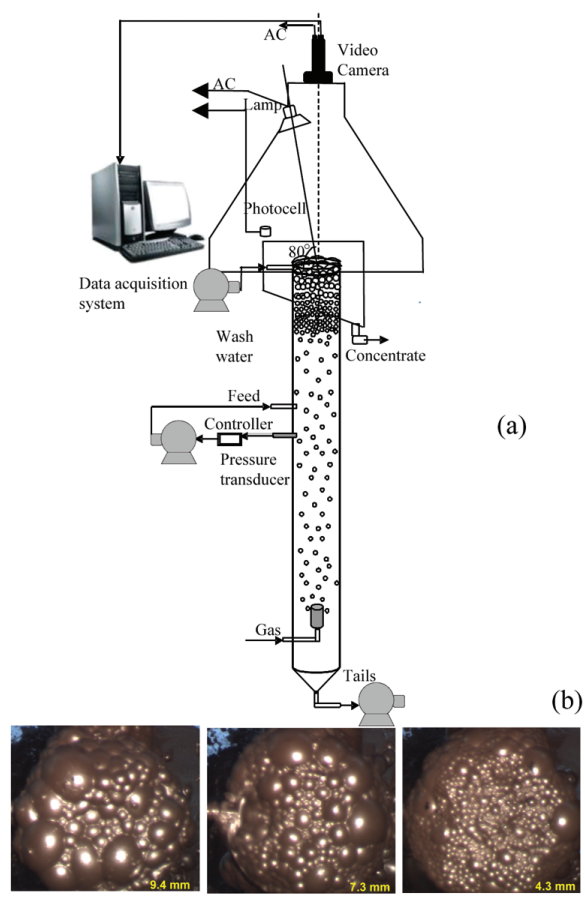

Figure 1—(a) Experimental set-up. (b) Typical froth images

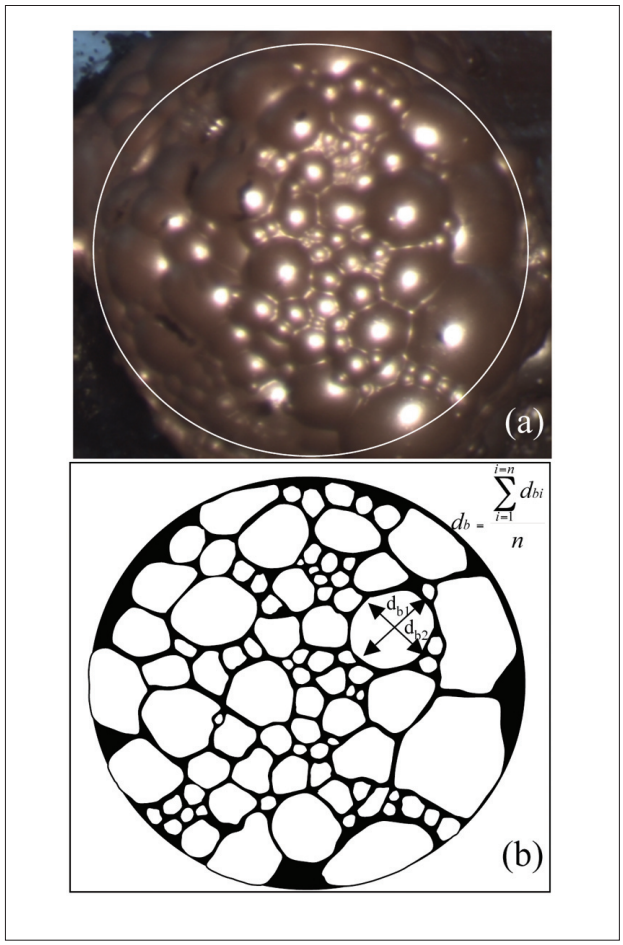

Figure 2—(a) Illustration of the method used to calculate the reference bubble diameter of the bubbles in the froth surface. (b) A high contrast image of the froth surface

measured bubble size distribution and the measured mean diameter of the image. This was a tedious stage and is not intended to be used as part of an online automatic method to estimate the bubble size distribution of froth surfaces.

Image Pro® software was also used to digitize the images and to obtain the numerical matrix and, together with the reference mean diameter, to compose the pattern that will be learned by the ANN. Each datum of the numerical matrix is proportional to the illumination of each pixel in the image, a value of zero for black and 255 for white. Only a section of each image with similar dimensions was selected for numerical analysis. It should be noted that each image produced a large numerical matrix, and therefore, in order to avoid extremely large files, only every other data point was selected. To take into account the information of the light intensity with which the images were acquired, an extra column was added to the numerical matrix of each digital image.

The architecture of the neural network trained in this work was fed forward with 153 inputs (digitalized pixels of a row of the image), one hidden layer with 138 neurons and one neuron at the output layer (bubble diameter). A sigmoid equation was used as the transfer function in each of the nodes, and a unitary bias was input into the hidden layer. The neural network training used a database containing 4 992 patterns and a back propagation algorithm to learn the relationships that exist between the inputs and the outputs.

Results

The mineralized froth images were obtained at different luminosity intensities, which were easily obtained by changing the lens aperture, in order to simulate external light intensity changes. Typical images are shown in Figure 3, clearly showing the gradation in the darkness of the images.

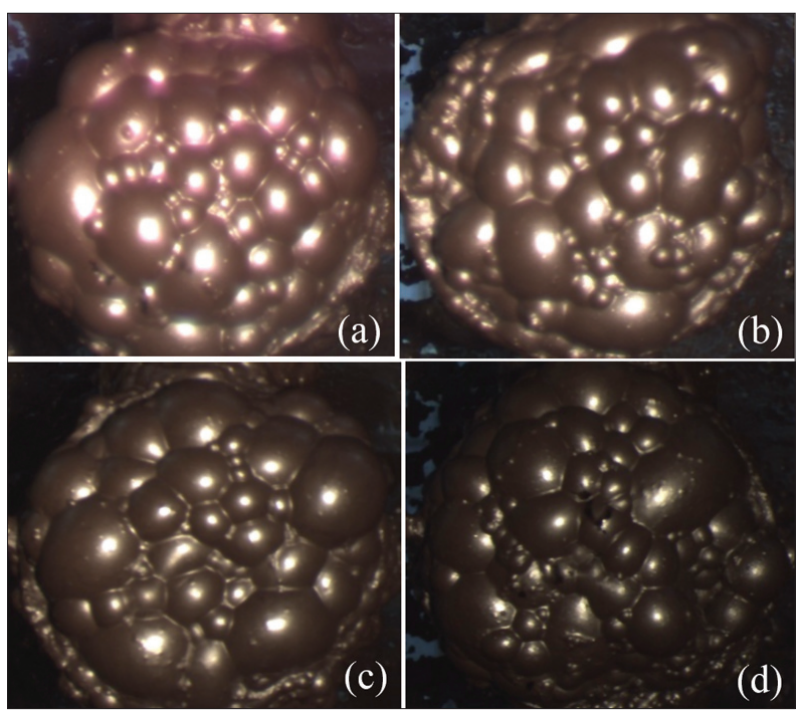

Figure 3—Images taken at different light intensities

Figure 4 shows that for each row of the digitalized image (i.e., a row of the numerical matrix), a brightness pattern exists (gray intensity versus pixel number). On examination of the figure, it is apparent that the intensity of the peaks denotes the brightness of the bubble and the amplitude is related to the bubble diameter. Comparing Figures 4(a) and 4(b), it is observed that the amplitude of the peaks and valleys are associated with the bubble diameter, whereas the number of peaks is associated with bubbles number. This type of pattern was interpreted by the neural model to estimate the bubble diameter.

The neural network estimates the average diameter for each input, i.e., for each row of the numerical matrix. After the neural network processing was completed for all the rows of an image, a number of estimated diameters were generated (see Figure 5 (a)). The reason is that for each image with a given mean diameter ($d_{b\ reference\ for\ image}$), several estimated diameters are calculated (see Figure 5(b)). The next step was to calculate the arithmetic mean of the estimated diameters. The explanation of this estimated diameter dispersion is that when one scans a row, a bubble is detected and the distance between its left and right limits is determined. However, this represents the diameter only if it cuts the bubble at its centre. When one scans the next row, the same bubble is observed but the distance between its left and right limits may be different from the one measured in previous row. As a consequence, a dispersion of the estimated bubble diameters is obtained.

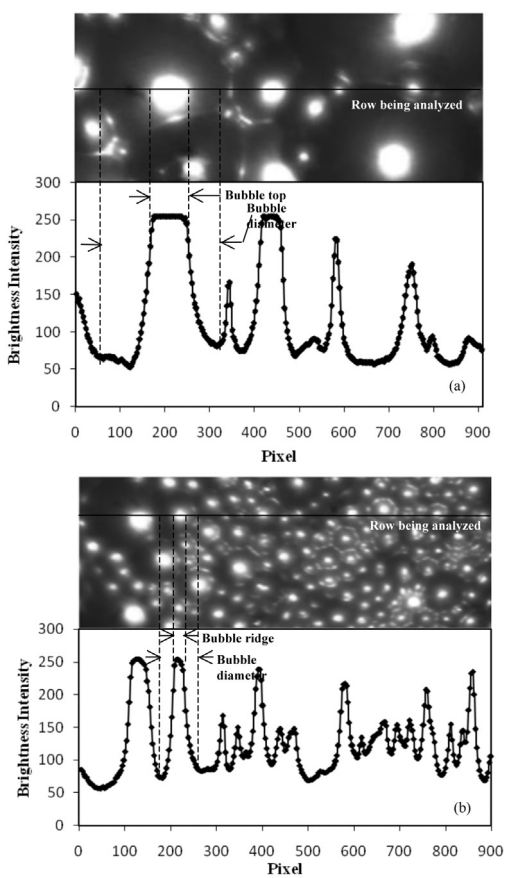

Figure 4—Brightness versus pixel number in a row of the digitalized images (input for ANN). (a) For large bubbles and (b) for small bubbles

Neural network performance with different lighting conditions

The first challenge was to test the ANN trained using images with different bubble diameters and a constant illumination intensity to predict the bubble diameters of images obtained with different illumination intensities. The results of this test contained errors, as the learned patterns (images with constant illumination) were not sufficient to interpret images obtained at different illumination intensities. For this analysis, the training was executed with a database of images with high light intensity, while the test performed predicts the mean bubble diameter of images of low illumination. Figure 6 (a) presents a significant dispersion between measured and estimated bubble diameters, even though the best results are those with higher illumination. Figure 6 (b) plots the correlation factor as a function of light intensity, showing a high correlation for images with smaller equivalent lens aperture. This is because the neural network model was trained to recognize images with high illumination intensity (i.e. smaller equivalent lens aperture), but it is unable to interpret images with different degrees of lighting.

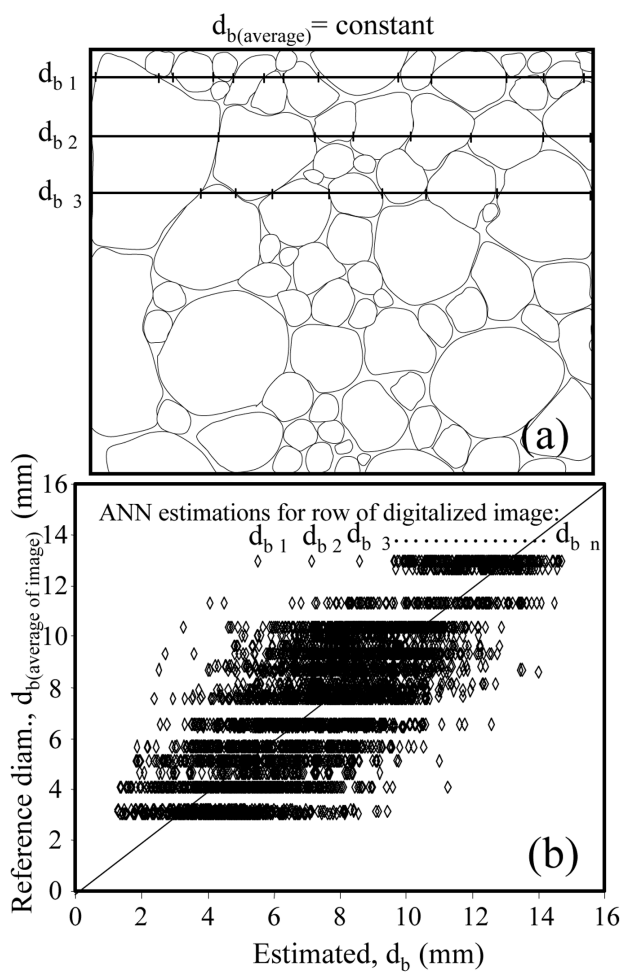

Figure 5—(a) Definition of the measured value of $d_{b(average\ of\ image)}$ and the estimated value of $d_{bn\ (ANN\ prediction\ for\ row)}$. (b) The actual estimated and measured diameters. Note that for any given measured value there are several estimated values (the same number of analysed rows)

Neural networks to estimate bubble diameter and bubble size distribution

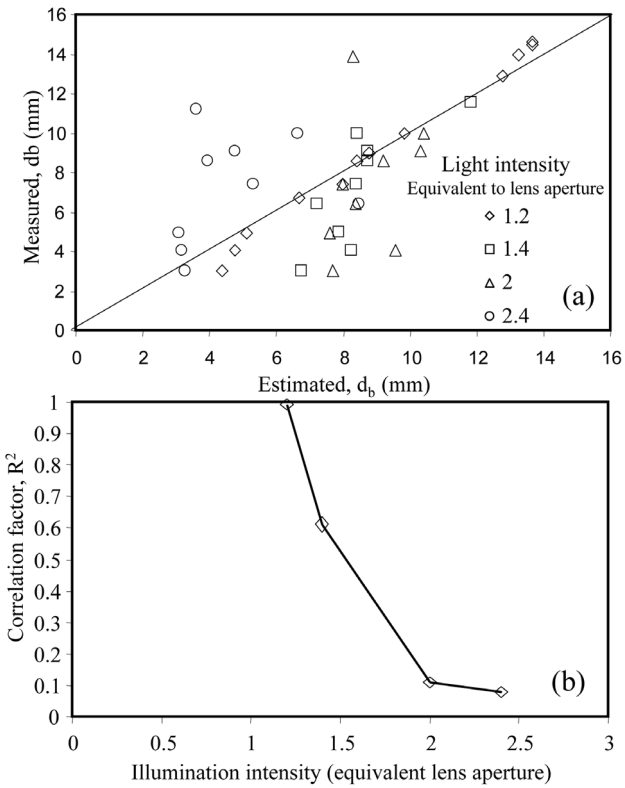

Figure 6—(a) Measured and estimated bubble diameters when ANN was trained with images of constant illumination and tested with images of different illumination intensities. (b) Correlation factor as a function of light intensity

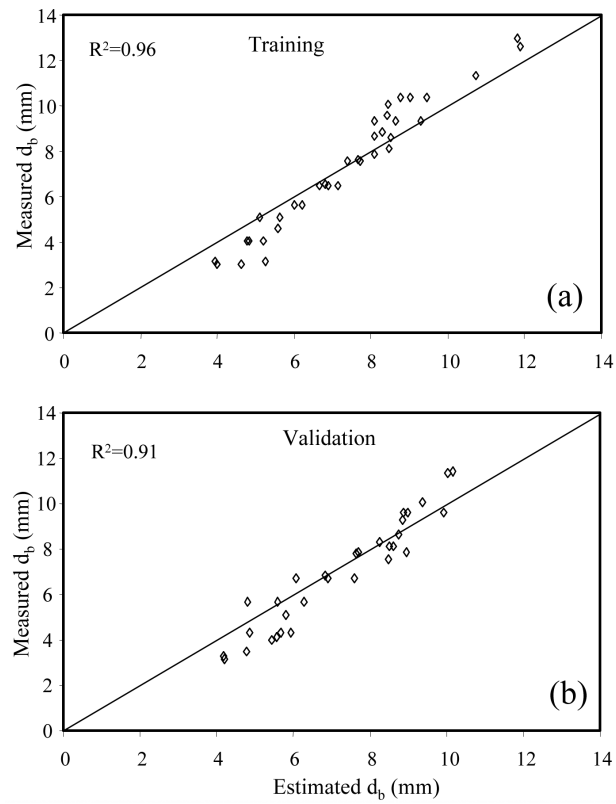

Figure 7—Correlation between measured and predicted bubble diameters. (a) Training results, and (b) validating results

The second test was to carry out ANN learning using images of froths with different grades of illumination, and with froth bubble diameters between 3 and 13 mm. In this case, the additional information included in the training pattern database was the lighting intensity, which is equivalent to the lens aperture. After this training, the ANN was used to predict bubble diameters from data contained in images that were not included in the training database. The assessed database included a numerical matrix comprising 4 992 rows and 153 columns.

Figure 7(a) shows a test of the training results, showing a high regression factor ($R^2 = 0.96$) between the predicted and the reference values. Nevertheless, the results of this figure should be interpreted with caution, since the training data and testing database were the same (5 622 patterns). Figure 7(b) shows the validation results, i.e., for a case where the test was accomplished using a different database (4 992 patterns) to that use training data. Again, the results show a high regression factor ($R^2 = 0.91$) between the measured and estimated diameters, allowing one to draw the conclusion that ANN is reliable enough for image analysis to predict froth diameters.

The bubble diameter distributions were obtained by taking into consideration the diameters estimated from the rows of the numerical matrix analysed by the ANN (see Figure 5). Figure 8 (a) shows three size distributions estimated by the model, and Figure 8 (b) shows the corresponding size distributions obtained manually. These

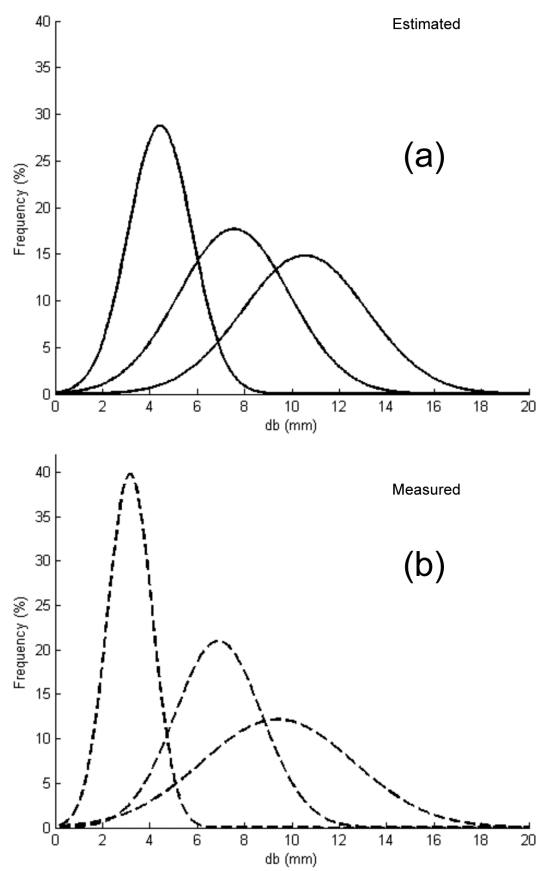

Figure 8—(a) Bubble size distribution estimated by ANN. (b) Bubble size distribution obtained by manual measurements

data were fitted to a Gaussian distribution for a better interpretation. Comparing Figures 8 (a, b), it is observed that even though bubble size distributions estimated and measured are similar, the measured ones are slightly smaller than the estimated ones. This bias is also observed in Figures 7 (a, b).

Conclusion

Neural network models can easily estimate the main bubble diameter and bubble size distribution of froth surfaces. In this application, it is important to convert the images from colour to gray scale, to normalize the information to be processed by the ANN. To achieve successful ANN training, it is necessary to have a large database that includes froth images with several different bubble diameter distributions. In addition, when large variations in luminosity are expected, the training database should contain information on the light intensity (e.g., the output of a photocell sensor in this work). Otherwise, the performance of ANN models is susceptible to error. The best results were obtained using an ANN with 153 inputs, a hidden layer with 138 neurons, a sigmoidal transfer function, and a unitary bias for each layer.

Acknowledgments

The authors are grateful to CONACYT (Mexico) for the funding received to conclude this work and to J. A. González for technical support in the laboratory.

References

1. Symonds, P.J. and De Jager, G. A technique for automatically segmenting images of the surface froth structures that are prevalent in flotation cells. *Proc. of the 1992 South African Symposium on Communications and Signal Processing*, University of Cape Town, Rondebosch, South Africa, 1992. pp. 111–115.
2. Woodburn, E.T., Austin, L.G., and Stockton, J.B. A froth based flotation kinetic model, *Trans. I ChemE*, 1994. 72A, pp. 211–56.
3. Moolman, D.W., Eksteen, J.J., Aldrich, C., and Van Deventer, J.S.J. The significance of flotation froth appearance for machine vision control. *Int. J. Mineral Processing*, vol. 48, 1996. pp. 135–158.
4. Hargrave, J.M. and Hall, S.T. Diagnosis of concentrate grade and mass flow rate in tin flotation from color and surface texture analysis. *Minerals Eng.*, vol. 10, no. 6, 1997. pp. 613–621.
5. Holtham, P.N. and Nguyen, K.K. On-line analysis of froth surface in coal and mineral flotation using JKFrothCam. *Int. J. Mineral Processing*, vol. 64, 2002. pp. 163–180.
6. Thomson, S., Fueten, F., and Bockus D. Mineral identification using artificial neural networks and the rotating polarizer stage, *Computers & Geosciences*, vol. 27, 2001. pp. 1081–1089.
7. Gupta, S., Liu P-H., Svoronos, S.A., Sharma, R., Abdel-Khalek, N.A., Cheng, Y., and El-Shall, H. Hybrid first-principles/neural networks model for column flotation. *AIChe Journal. AIChe Journal*, vol. 45, no. 3, 1999. pp.557–566.
8. Shumsher-Rughooputh, H.C. and Daharam-Vir, S.D. Neural network process vision systems for flotation process. *Neural network process vision systems,* vol. 31, no. 3/4, 2002. pp. 529–535.
9. Grau, R.A. and Heiskanen, K. Visual techniquefor measuring bubble size in flotation machines. *Minerals Engineering*, 2002. pp. 507–513.
10. Hernández-Aguilar, J.R., Coleman, R.G., Gomez, C.O., and Finch, J.A.A. comparation between capilarity and imaging techniques for sizing bubbles in flotation systems. *Mineral Engineering,* vol. 17, 2004. pp. 53–61. ◆